Supplementary Materials

Article

NiO/TiO_2 p-n Heterojunction Induced by Radiolysis for Photocatalytic Hydrogen Evolution

Ana Andrea Méndez-Medrano [1,2], Xiaojiao Yuan [1,†], Diana Dragoe [3], Christophe Colbeau-Justin [1], José Luis Rodríguez López [2,‡] and Hynd Remita [1,*]

[1] Institut de Chimie Physique, UMR 8000 CNRS, Université Paris-Saclay, 91405 Orsay, France; hynd.remita@universite-paris-saclay.fr
[2] Advanced Materials Department, Instituto Potosino de Investigación Científica y Tecnológica, A.C., IPICYT, San Luis Potosí 78216, SLP, México; andy-mm@live.com
[3] Institut de Chimie Moléculaire et des Matériaux d'Orsay, UMR 8182 CNRS, Université Paris-Saclay, 91405 Orsay, France; diana.dragoe@universite-paris-saclay.fr
* Correspondence: hynd.remita@universite-paris-saclay.fr
† Current address: Department of Chemistry, ICIQ, Institute of Chemical Research of Catalonia, 43007 Tarragona, Spain.
‡ Current address: Circ. Jardines de los Pinos, Jardines de Jacarandas, San Luis Potosí 78136, SLP, Mexico.

Table S1. Doses for the modified samples.

Sample	Concentration (M)	Dose (kGy)
0.1 wt.% Ni/TiO_2	5.5×10^{-5}	0.4
0.5 wt.% Ni/TiO_2	2.7×10^{-4}	1.8
1.0 wt.% Ni/TiO_2	4.5×10^{-4}	2.9
3.5 wt.%. Ni/TiO_2	1.8×10^{-3}	11.6
5.0 wt.%. Ni/TiO_2	2.2×10^{-3}	14.08

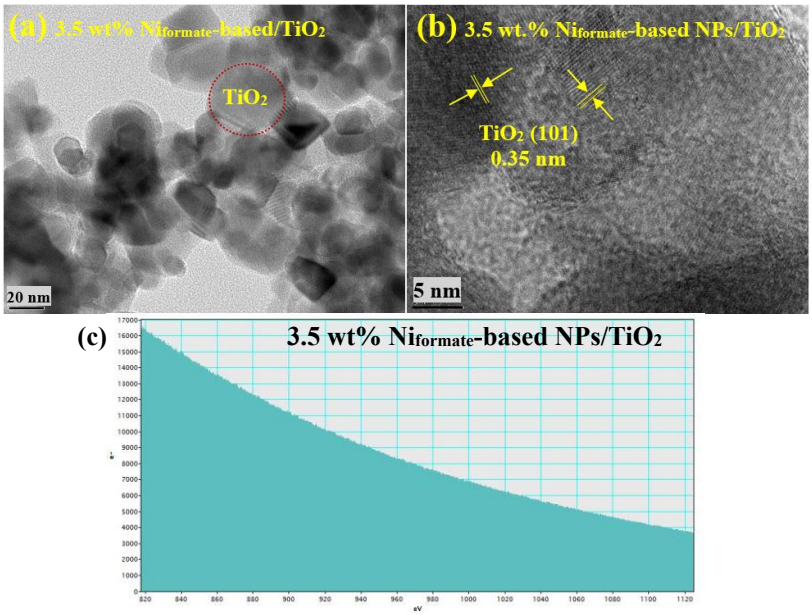


Figure S1. (a) TEM micrograph, (b) HRTEM micrograph, and (c) EELS spectrum of 3. 5 wt.% $Ni_{formate}$-based NPs/TiO_2.

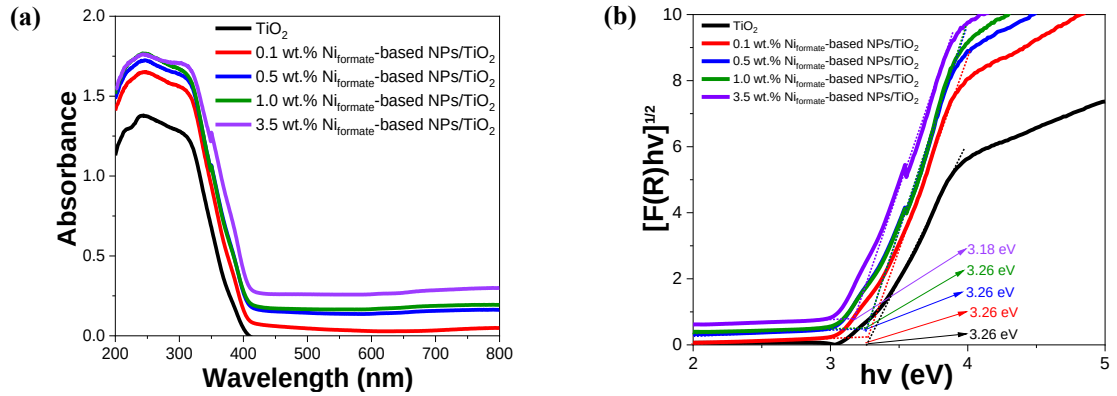


Figure S2. (a) DRS spectra and their (b) Tauc plot of $Ni_{formate}$-based NPs/TiO_2-modified samples and bare TiO_2.

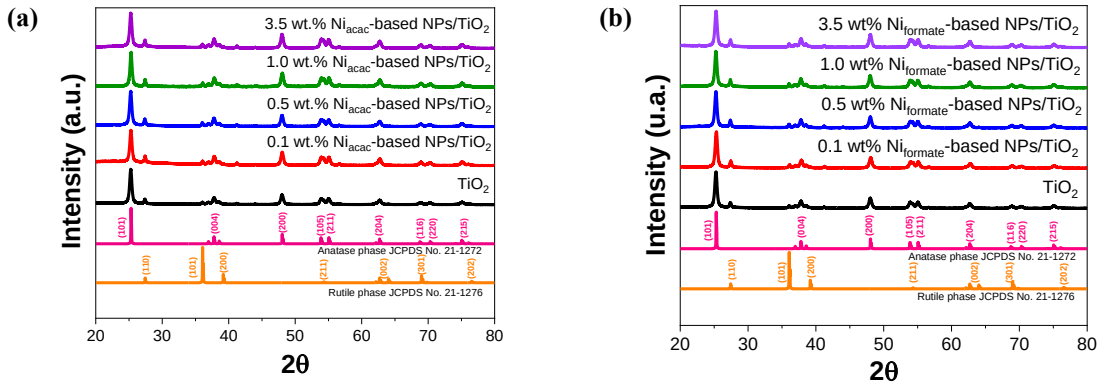


Figure S3. X-ray diffraction (XRD) patterns of (a) $Ni_{formate}$-based NPs/TiO_2 and (b) Ni_{acac}-based NPs/TiO_2-modified samples and bare TiO_2 with the reference peaks of the anatase and rutile crystalline phases.

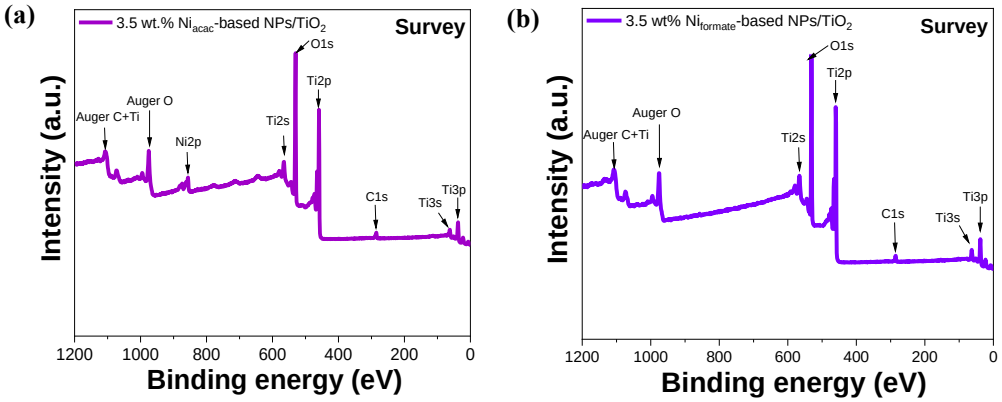


Figure S4. Survey XPS spectra of (a) 3.5wt% Ni$_{acac}$-based NPs/TiO$_2$ and (b) 3.5wt% Ni$_{formate}$-based NPs/TiO$_2$ samples.

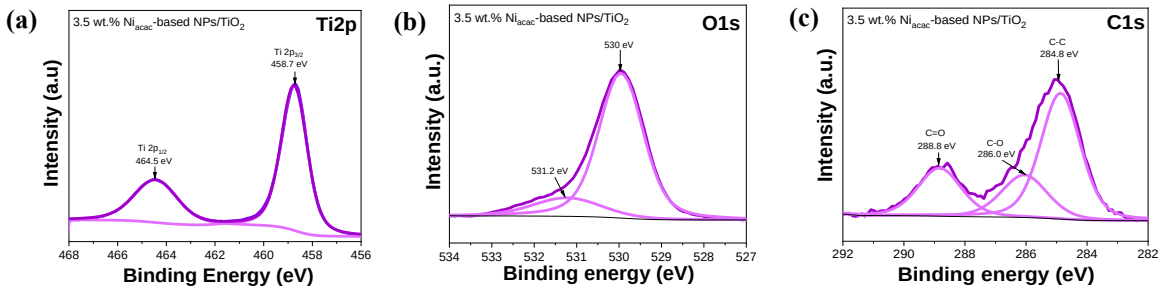


Figure S5. Narrow-scan XPS spectra of (a) Ti *2p*, (b) O *1s*, and (c) C *1s* of 3.5wt% Ni$_{acac}$-based NPs/TiO$_2$-modified sample.

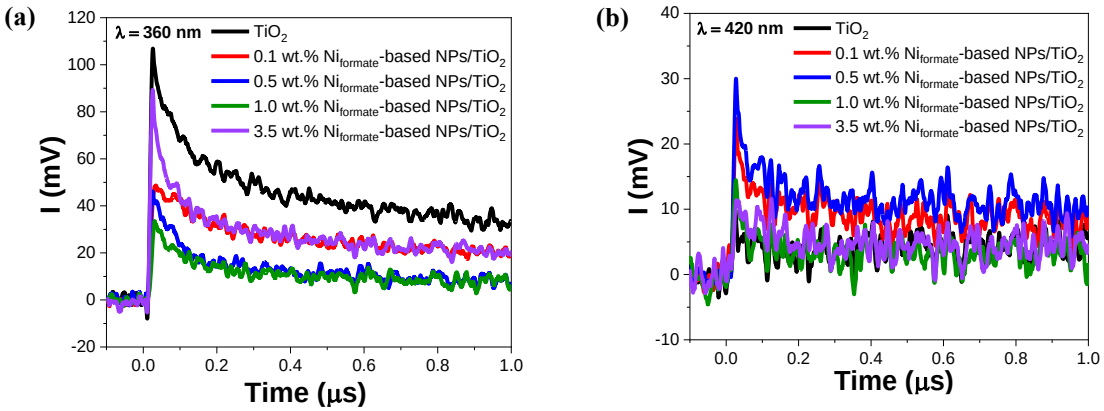


Figure S6. TRMC signals of Ni$_{formate}$-based NPs/TiO$_2$-modified samples and bare TiO$_2$ at different wavelengths: (a) λ=360 nm and (b) λ=420 nm. The laser energy of these wavelengths was 1.1 and 2.3 mJ, respectively.

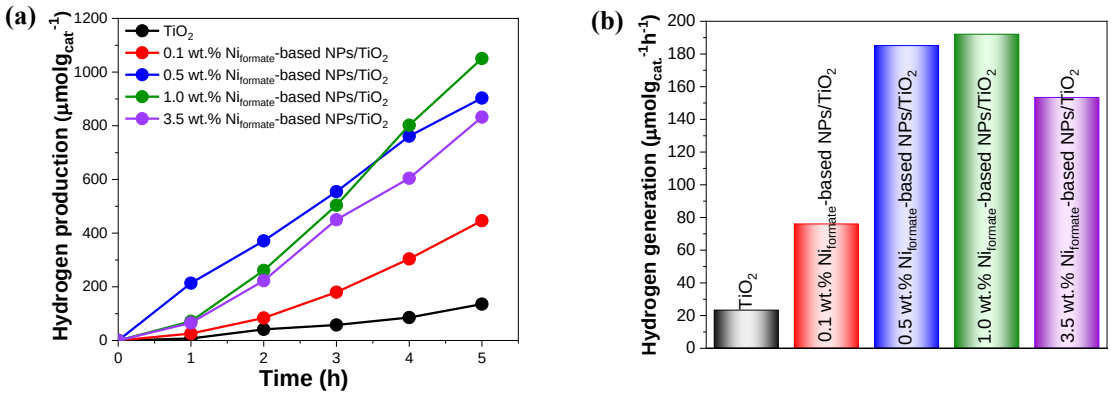


Figure S7. (a) Photocatalytic hydrogen generation for $Ni_{formate}$-based NPs/TiO_2 samples and bare TiO_2 under UV–visible light, and (b) their hydrogen generation rates (μmol $g_{cat.}^{-1}$ h^{-1}) under UV–visible light irradiation from 25% v/v methanol aqueous solution.

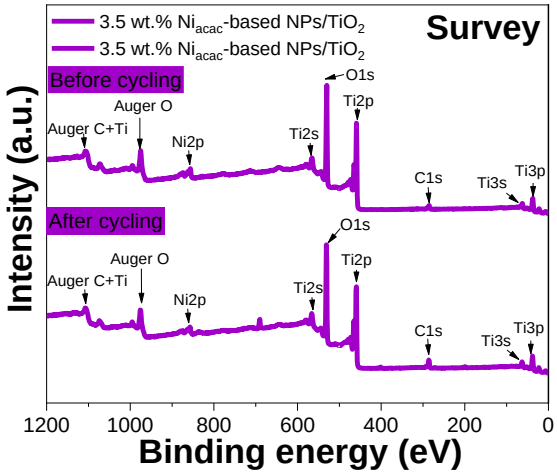


Figure S8. Survey XPS spectra of 3.5 wt.% Ni_{acac}-based NPs/TiO_2 sample before and after cycling.

Table S2. Comparison of hydrogen generation under UV–visible light of the different photocatalysts.

Samples	Scavenger	Lamp	Hydrogen generation UV–visible	Hydrogen generation UV	Hydrogen generation Visible	Reference
3.5 wt.% Ni-NPs/TiO_2	25% v/v methanol/water	Hg lamp	998.4 μmol $g_{cat.}^{-1}$ h^{-1} ~42-fold higher than TiO_2		1.5 μmol $g_{cat.}^{-1}$ h^{-1}	Our work
Ni/TiO_2	25% v/v methanol/water	Solarium Philips HB175 lamp Maximum peak at 365 nm		260.76 μmol h^{-1}		[1]
0.32 mol% Ni/TiO_2	25% v/v methanol/water	UV-LEDs at 365 nm	2547 μmol $g_{cat.}^{-1}$ h^{-1} ~135-fold than TiO_2			[2]
NiO/rGO/TiO_2	80 mL H_2O: 20 mL methanol	Solar simulator 300 W equipped with Xe lamp as source	240 μmol/h/g			[3]
2.0 wt % $Ni(OH)_2$/TiO_2 nanotubes	5% v/v crude glycerol/water	Solar light	4719 μmol$g_{cat.}^{-1}h^{-1}$ ~12-fold higher than TiO_2		0	[4]
Ni/C/TiO_2	80 mL H_2O: 20 mL methanol	300 W Xe lamp	1745 μmol$g_{cat.}^{-1}h^{-1}$ ~9-fold than TiO_2			[5]
1 wt% NiO/TiO_2	methanol/H_2O (1:1 v:v)	1. 6W Hg vapor light source wavelength range: 320-400 nm		2693 μmol $g_{cat.}^{-1}$ h^{-1}		[6]
0.5 wt% Ni/TiO_2-P25	Glycerol (10 vol%)	UV lamp at 365 nm		26000 μmol $g_{cat.}^{-1}h^{-1}$ >24 h		[7]
1.5 wt% NiO/TiO_2	200 mL water: 20 mLof methanol	300 W high-pressure Hg lamp		162. 6 μmol h^{-1}		[8]
NiO/CdS	100 mL of aqueous solution containing 30 mL methanol	Xe lamp (300 W) filter ($\lambda > 400$ nm)			445.6 μmol h^{-1} 41 times higher than CdS 5 h	[9]
Ni/GO-CdS	Ethanol:water (50/50 vol%)	4 LED lamps of λ=450 nm (4W each)			8866 μmol $g_{cat.}^{-1}$ h^{-1}	[10]
$Ni(OH)_2$-CdS/g-C_3N_4	20 mL aqueous solution containing Na_2S and Na_2SO_3	300 W Xe lamp 420 nm cut-off filter			115.18 μmol $mg_{cat.}^{-1}$ h^{-1}	[11]

References

1. Melián, E. P.; Suárez, M. N.; Jardiel, T.; Rodríguez, J. M. D.; Caballero, A. C.; Araña, J.; Calatayud, D. G.; Díaz, O. G. Influence of nickel in the hydrogen production activity of TiO_2. *Appl. Catal. B* **2014**, *152-153*, 192-201. DOI: 10.1016/j.apcatb.2014.01.039

2. Wang, W.; Liu, S.; Nie, L.; Cheng, B.; Yu, J. Enhanced photocatalytic H_2-production activity of TiO_2 using $Ni(NO_3)_2$ as an additive. *Phys. Chem. Chem. Phys.* **2013**, *15*, 12033–12039. DOI: 10.1039/c2cp43628k

3. Yu, X.; Zhang, J.; Zhao, Z.; Guo, W.; Qiu, J.; Mou, X.; Li, A.; Claverie, J. P.; Liu, H. NiO-TiO_2 p-n heterostructured nanocables bridged by zero-bandgap rGO for highly efficient photocatalytic water splitting. *Nano Energy* **2015**, *16*, 207-217. DOI: 10.1016/j.nanoen.2015.06.028

4. Lakshmana Reddy, N., Cheralathan, K. K., Durga Kumari, V., Neppolian, B., Muthukonda Venkatakrishnan, S. Photocatalytic Reforming of Biomass Derived Crude Glycerol in Water: A Sustainable Approach for Improved Hydrogen Generation Using $Ni(OH)_2$ Decorated TiO_2 Nanotubes under Solar Light Irradiation. *ACS Sustain. Chem. Eng.*, **6**, 3754, (2018). DOI: 10.1021/acssuschemeng.7b04118

5. Zhao, X.; Xie, W.; Shao, X.; Wang, Z.; Yang, B.; Yang, C.; Wang, J.; Su, X. An effective Ni/C co-catalyst for promoting photocatalytic hydrogen evolution over TiO_2 nanospheres. *Mater. Sci. Semicond. Process.* **2022**, *148*, 106775. DOI: 10.1016/j.mssp.2022.106775

6. Uddin, M. T.; Nicolas, Y.; Olivier, C.; Jaegermann, W.; Rockstroh, N.; Junge, H.; Toupance, T. Band alignment investigations of heterostructure NiO/TiO_2 nanomaterials used as efficient heterojunction earth-abundant metal oxide photocatalysts for hydrogen production. *Phys. Chem. Chem. Phys.* **2017**, *19*, 19279-19288. DOI: 10.1039/c7cp01300k

7. Chen, W. T.; Chan, A.; Sun-Waterhouse, D.; Llorca, J.; Idriss, H.; Waterhouse, G. I. N. Performance comparison of Ni/TiO_2 and Au/TiO_2 photocatalysts for H_2 production in different alcohol-water mixtures. *J. Catal.* **2018**, *367*, 27–42. DOI: 10.1016/j.jcat.2018.08.015

8. Sreethawong, T.; Suzuki, Y.; Yoshikawa, S. Photocatalytic evolution of hydrogen over mesoporous TiO_2 supported NiO photocatalyst prepared by single-step sol-gel process with surfactant template. *Int. J. Hydrog. Energy* **2005**, *30*, 1053-1062. DOI: 10.1016/j.ijhydene.2004.09.007

9. Chen, X.; Chen, W.; Lin, P.; Yang, Y.; Gao, H.; Yuan, J.; Shangguan, W. In situ photodeposition of nickel oxides on CdS for highly efficient hydrogen production via visible-light-driven photocatalysis. *Catal. Commun.* **2013**, *36*, 104–108. DOI: 10.1016/j.catcom.2013.03.016

10. Quiroz-Cardoso, O.; Oros-Ruiz, S.; Solís-Gómez, A.; López, R.; Gómez, R. Enhanced photocatalytic hydrogen production by CdS nanofibers modified with graphene oxide and nickel nanoparticles under visible light. *Fuel* **2019**, *237*, 227–235. DOI: 10.1016/j.fuel.2018.10.013

11. Yan, Z.; Sun, Z.; Liu, X.; Jia, H.; Du, P. Cadmium sulfide/graphitic carbon nitride heterostructure nanowire loading with a nickel hydroxide cocatalyst for highly efficient photocatalytic hydrogen production in water under visible light. *Nanoscale* **2016**, *8*, 4748–4756. DOI: 10.1039/c6nr00160b